NOE-Derived Solution Structures of a Benzylborato−Azasilazirconacyclobutane Complex, {(Me$_3$Si)$_2$N}Zr(CH$_2$SiMe$_2$NSiMe$_3$){η^6-PhCH$_2$B(C$_6$F$_5$)$_3$}

J. Monty Wright,[†,§] Clark R. Landis,*[,†] Marianne A. M. P. Ros,*[,‡] and Andrew D. Horton[‡]

Department of Chemistry, University of Wisconsin, Madison, Wisconsin 53706, and Shell International Chemicals, B.V., Amsterdam (CTANL/3), P.O. Box 38000, 1030 BN Amsterdam, The Netherlands

Received July 7, 1998

The benzylborato−azasilazirconacyclobutane complex **1** was formed by ligand cyclometalation upon reaction of {(Me$_3$Si)$_2$N}$_2$Zr(CH$_2$Ph)$_2$ with B(C$_6$F$_5$)$_3$. Quantitative analysis of the ^{1}H NOESY time course of **1** using the conformer population analysis method demonstrates that the dominant conformers in solution are rapidly exchanging benzyl borate rotamers, closely bound to the asymmetric zirconium. The ring rotates such that the benzylic methylene eclipses the metallocyclobutylmethylene in the majority of the population and the free amide nitrogen in the minority of the population. A molecular dynamics approach was required to solve this solution structure because a mixture of static conformations does not satisfactorily explain the observed spectra.

Introduction

The polymerization of alkenes as catalyzed by group IV transition metal complexes continues to be an active area of research and commercial development.[1,2] A recent trend in catalyst development is the substitution of the metallocene cyclopentadienyl ligands with other functional groups. A variety of diamide catalysts recently have been produced,[3−12] including that produced by Shell[13] which is the focus of this work. This work describes part of an effort to expand on that success by understanding the solution structure of {(Me$_3$Si)$_2$N}Zr(CH$_2$SiMe$_2$NSiMe$_3$){η^6-PhCH$_2$B(C$_6$F$_5$)$_3$} (**1**) as a presumed catalyst precursor. The catalyst, **1**, initiates polymerization of ethylene slowly, possibly because the binding strength of the borate ligand hinders the formation of the active catalysts.[14] The synthesis of **1** has been described in detail in ref 14, and Scheme 1 illustrates the essentials of its preparation. η^6-Arene binding to group IV metals is well precedented. Examples span simple arene coordination,[15−17] the coordination of aryl borates,[18−21] and the coordination of benzylic borates[16,22,23] similar to the mode proposed for **1**.

Structural tools, such as NOESY (nuclear Overhauser effect spectroscopy) methods, potentially provide valuable probes of the solution structures of organometallics, provided that the data can be modeled realistically and efficiently. The primary goal of this research is to use solution NMR methods and multiconformational analysis to probe the three-dimensional structure of **1**. For this complex we focus on detailing the primary ring rotamers and the conformation of the zirconacyclobutane ring. Second, we are interested in pushing forward new algorithms for the modeling of small molecule NOE (nuclear Overhauser effect) data such as the 2DCPA (2-dimensional conformer population analysis).[24−27]

[†] University of Wisconsin.
[§] Current address: Kodak Company, 1700 Dewey Ave., Rochester, NY 14650-1860.
[‡] Shell International Chemicals.

(1) Reisch, M. S. *Chem. Eng. News* **1997**, *75*, 14−16.
(2) Kaminsky, W.; Arndt, M. *Adv. Polym. Sci.* **1997**, *127*, 143−187.
(3) Baumann, R.; Davis, W. M.; Schrock, R. R. *J. Am. Chem. Soc.* **1997**, *119*, 3836.
(4) Male, N. A. M.; Thornton-Pett, M.; Bochmann, M. *J. Chem. Soc., Dalton Trans.* **1997**, 2487.
(5) Jäger, F.; Rösky, H. W.; Dorn, H.; Shah, S.; Noltemeyer, M.; Schmidt, H.-G. *Chem. Ber.* **1997**, *130*, 399.
(6) Scollard, J. D.; McConville, D. M. *J. Am. Chem. Soc.* **1996**, *118*, 10008.
(7) Scollard, J. D.; McConville, D. M.; Payne, N. C.; Viltal, J. J. *Macromolecules* **1996**, *29*, 5241.
(8) Scollard, J. D.; McConville, D. M.; Rettig, S. J. *Organometallics* **1997**, *16*, 1810.
(9) Shah, S. A.; Dorn, H.; Voight, A.; Rösky, H. W.; Parsini, E.; Schmidt, H.-G.; Noltemeyer, M. *Organometallics* **1996**, *15*, 3176.
(10) Fuhrmann, H.; Brenner, S.; Arndt, P.; Kempe, R. *Inorg. Chem.* **1996**, *35*, 6742.
(11) Sasaki, T.; Shiraighi, H.; Johoji, H.; Katayama, H. In Eur. Pat. Appl., Sumitomo, 1993.
(12) Canich, J. M.; Turner, H. W. Exxon: World Pat. Appl., 1992.
(13) Horton, A. D.; de With, J.; van der Linden, A. J.; van de Weg, H. *Organometallics* **1996**, *15*, 2672−2674.
(14) Horton, A. D.; de With, J. *J. Chem. Soc., Chem. Commun.* **1996**, 1375−1376.
(15) Gillis, D. J.; Tudoret, M.-J.; Baird, M. C. *J. Am. Chem. Soc.* **1993**, *115*, 2543.
(16) Pellecchia, C.; Grassi, A.; Immirzi, A. *J. Am. Chem. Soc.* **1993**, *115*, 1160.
(17) Lancaster, S. J.; Robinson, O. B.; Bochmann, M.; Coles, S. J.; Hursthouse, M. B. *Organometallics* **1995**, *14*, 2456.
(18) Horton, A. D.; Fryns, J. H. G. *Angew. Chem., Int. Ed. Engl.* **1991**, *30*, 1152.
(19) Bochmann, M.; Karger, G.; Jagger, A. J. *J. Chem. Soc., Chem. Commun.* **1990**, 1038.
(20) Bochmann, M.; Jaggar, A. J.; Nicholls, J. C. *Angew. Chem., Int. Ed. Engl.* **1990**, *29*, 780.
(21) Schaverien, C. J. *Organometallics* **1992**, *11*, 3476.
(22) Pellecchia, C.; Immirzi, A.; Grassi, A.; Zambelli, A. *J. Am. Chem. Soc.* **1993**, *115*, 4473.
(23) Pellecchia, C.; Grassi, A.; Zambelli, A. *J. Mol. Catal.* **1993**, *82*, 57.
(24) Casey, C. P.; Hallenbeck, S. L.; Wright, J. M.; Landis, C. R. *J. Am. Chem. Soc.* **1997**, *119*, 9680−9690.

10.1021/om980571o CCC: $15.00
Publication on Web 10/16/1998

Scheme 1

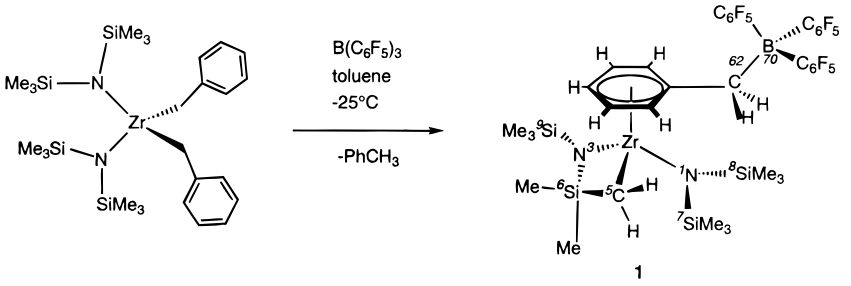

1

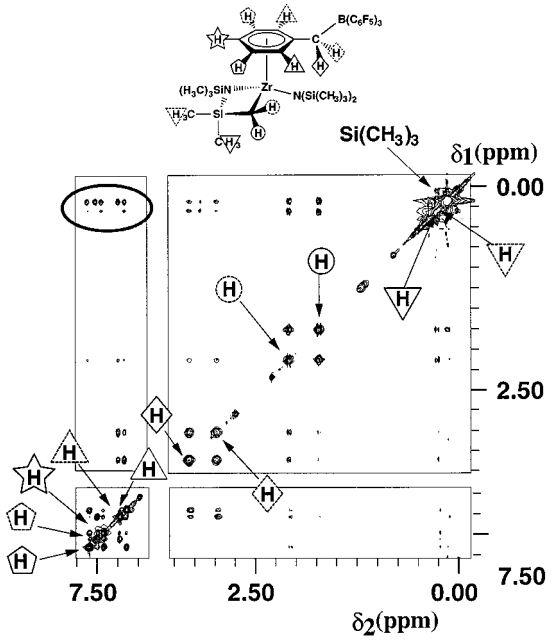

Figure 1. ^{1}H NOESY spectrum of $\{(Me_3Si)_2N\}Zr(CH_2SiMe_2NSiMe_3)\{\eta^6\text{-}PhCH_2B(C_6F_5)_3\}$ (**1**) in $CDCl_2CDCl_2$ at −20 °C (t_m = 300 ms) displayed in a tiled format. The ellipse in the upper left corner highlights cross-peaks between the arene protons and the trimethylsilylamido group of the metallacylic ring.

Results and Discussion

A ^{1}H NOESY spectrum of zirconium benzylborato-azasilacyclobutane complex **1** taken with a 300 ms mixing time is shown in Figure 1 as a contour plot. In this spectrum the off-diagonal peaks indicate NOE interactions between the corresponding protons; the magnitudes of the cross-peaks are related to the conformationally averaged distances between the protons. Qualitiatively, the NOESY spectrum exhibits good dispersion and well-resolved peaks; only the terminal trimethylsilyl groups are overlapped. The identities of the ortho, meta, and para arene hydrogens are readily apparent from both their cross-peaks with each other and from the cross-peaks of the ortho protons with the diastereotopic benzylic protons. Similarly, NOE cross-peaks uniquely determine the identities of each diastereotopic methylene proton and each diastereotopic $SiMe_2$−methyl resonance of the four-membered metallacyclic ring. Just one member of each of these diastereotopic pairs exhibits a substantial cross-peak with the benzylic protons. Qualitatively, the NOESY spectrum suggests that the Zr-bound arene ring has some freedom to rotate about the Zr-centroid axis: the trimethylsilyl groups exhibit large cross-peaks to *all* arene resonances as emphasized in the highlighted, upper left portion of the spectrum in Figure 1. If the arene ring were static, simple models indicate that fewer cross-peaks would be observed. These qualitative observations indicate that realistic analysis of the NOE data requires a multiconformational approach.

The solution structure of **1** was determined by analyzing the time course of the quantitative ^{1}H 2D NOESY data with the multiconformational analysis technique, 2DCPA.[24−27] The 2DCPA method correlates the distance-related information obtained from the buildup of NOE intensities to the NOE intensities calculated for a large set of energetically feasible model conformations generated by molecular mechanics (MM). The 2DCPA analysis seeks the smallest combination of conformers that best accounts for all the experimental NOE data. Our approach to analyzing the solution conformations of **1** takes advantage of several distinctive features of the 2DCPA method: (1) because the model is multiconformational, one is not forced to describe the structure with a single, averaged conformation, (2) the method employs full-relaxation matrix analysis with accurate simulation of spin-diffusion, (3) all data, including the absence of NOE cross-peaks, are quantitatively analyzed, and (4) the goodness-of-fit is determined by direct comparison of observed data (the time course of NOE intensities) with simulated data.

There are four steps in our use of the 2DCPA method: (1) quantitation of the NOESY peak volumes at all mixing times, (2) creation of an ensemble of possible static solution structures using molecular mechanics methods, (3) quantitative simulation of the complete NOESY time courses for different combinations of structures, and (4) further refinement by dynamics simulations of local motions on the 10 ps time scale for the best candidates from step 3.

NOE Data Collection. ^{1}H NOESY spectra were collected in tetrachloroethane-d_2 at −20 °C using six different mixing times. An example ^{1}H NOESY spectrum with a mixing time of 200 ms is shown in Figure 1. As Figure 1 demonstrates, all seven unique benzyl resonances are clearly resolved and exhibit numerous cross-peaks with remaining resonances. Further details of the spectral workup are given in the Experimental Section.

Preliminary Structural Models. Our analysis assumes an η^6 coordination geometry for the benzyl borate

(25) Giovannetti, J. S.; Kelly, C. M.; Landis, C. R. *J. Am. Chem. Soc.* **1993**, *115*, 4040−4057.
(26) Landis, C. R.; Allured, V. S. *J. Am. Chem. Soc.* **1991**, *113*, 9493−9499.
(27) Landis, C. R.; Luck, L. L.; Wright, J. M. *J. Magn. Reson., Ser. B* **1995**, *109*, 44−59.

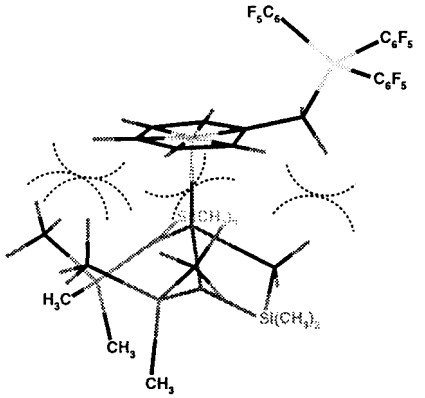

Figure 2. van der Waals contacts between the hydrogens of the benzylborate and the silylmethyls create "gears".

to construct the conformational ensembles. This assumption is consistent with available crystallographic data on η^6 arene analogues (vide infra), the observation of large changes in ^{19}F NMR chemical shifts,[14] and qualitative assessment of the one- and two-dimensional ^{1}H NMR; however, no additional experiments have been done to rule out other coordination modes.

Structural features of **1** that were not clear at the outset included the distance from the zirconium to the coordinated arene, the configuration and extent of pyramidalization of the silylamide nitrogens, and the orientation of the benzyl borate ligand with respect to the amide ligands. The initial static ensemble was 17 conformations selected from each of 12 classes of model conformations spanning a range of Zr to the benzyl centroid dummy atom (DA) distances, inversions of the silylamide nitrogens, and rotamers that move nonequivalent hydrogens, for a total of 204 conformations.

Significant Borate Conformational Motifs. Several interesting features of the models of **1** were discovered during the creation of the static ensemble. The most significant of these arise from the steric crowding that occurs when the silylmethyls are close to each other or to the benzylic ring hydrogens of the borate. Observation of the models during torsional searching, minimization, and subsequent molecular dynamics suggests that in some conformations the silyl methyl rotations are "geared" both among themselves and in a cogwheel fashion with the aryl hydrogens of the borate, as illustrated in Figure 2.

Three distinct aspects of the benzylborate anion conformation arose during the creation of the static ensemble. The first and most important aspect of the benzylborate anion conformation arises from rotation about the metal−aryl bond. This rotation is described by what will be defined as the benzyl ring torsion, and it turns out to be the largest single factor in the fit of calculated to observed NOESY data. It is fortunate that the presence of the stereogenic Zr in **1** makes all protons of the benzyl group chemically inequivalent (see Figure 1), which yields more useful NOE data. The distribution of benzyl torsions in the static ensemble is illustrated in Figure 3.

The second notable aspect of the benzylborate anion conformation is that the perfluorophenyl rings are correlated in their rotation and adopt a hybrid of a helical "propeller" and Mislow's one-ring flip conformations.[28] In the example shown in Figure 4 two of the phenyls have similar values for ω, $\omega_1 \approx \omega_3$, while for the third ring $\omega_2 \approx 0°$ (180°). Using this example labeling, ψ is such that the ortho fluorine of ring 2 fits into one of the three steric gaps around the benzylic methylene, that is, between the methylene hydrogen and the ortho benzylic hydrogen cis to it, or between the two methylene hydrogens. The perfluorophenyl ring that eclipses the benzyl ring has an ω torsion close to 90°(270°), putting the two rings as close to parallel and π-stacked as possible. A sampling of both *M* and *P* atropisomers[29] is included in the static ensemble.

The third important descriptor of benzylborate conformation is the ϕ torsion angle, which describes rotation about the ipso benzylic C−C bond. MM search results suggest there is an interaction between ψ and ϕ torsions that is illustrated in Figure 5. Note that when the perfluorophenyl ring with $\omega \approx 0°$ (180°) is trans to the benzyl ring, one of its ortho fluorines is between the two methylene hydrogens. This conformation keeps the methylene hydrogens approximately equidistant from the benzylic ring plane. When a perfluorophenyl ring eclipses the benzylic ring, one methylene hydrogen is nearly in the benzylic ring plane, and the other is substantially closer to the zirconium. With only two exceptions, the conformations in the static ensemble minimized so that ϕ was 90° (from the benzyl ring plane) or less in the direction of the ϕ arrow in Figure 4 and Figure 5.

Significant Silylamide Conformational Motifs. Silylamides have been studied extensively and are usually near planar about the N (i.e., improper torsions close to 0°), especially when coordinated to transition metals.[30,31] π-Bonding (N $p_\pi \rightarrow$ Si σ^*_π and N $p_\pi \rightarrow$ Zr d_π) back-bonding was modeled in this work by using bond orders of 1.5 and 1.25 for N−Zr and N−Si bonds, respectively. Although the nitrogen−metal bond is likely to have the smaller amount of p character in actuality,[32] the bond orders used represent a compromise to obtain bond lengths around nitrogen that match the crystal structures of close analogues. These findings suggested that at least some conformers in the ensemble needed to have a smaller improper torsion angle than the default. A search of the Cambridge Structural Database[33] revealed three Zr−silylamides, two of which were azasilazirconacyclobutanes. The structures have a median improper torsion angle of 13° for nitrogen in the azasilazirconacyclobutane and 3° for the nitrogen of the acyclic amide.[34]

Conformer Populations by Exhaustive Fitting. Given the ensemble of reasonable structures, the next

(28) Mislow, K. *Acc. Chem. Res.* **1976**, *9*, 26−33.
(29) Eliel, E. L.; Wilen, S. H.; Mander, L. N. *Stereochemistry of Organic Compounds*; Wiley-Interscience: New York, 1993.
(30) Ebsworth, E. A. V. *Volatile Silicon Compounds*; Pergamon Press: Oxford, 1963.
(31) Cotton, F. A.; Wilkinson, G. *Advanced Inorganic Chemistry*, 5th ed.; Wiley-Interscience: New York, 1988.
(32) Green, J. C.; Payne, M.; Seddon, E. A.; Andersen, R. A. *J. Chem. Soc., Dalton Trans.* **1982**, 887−892.
(33) Allen, F. H.; Kennard, O. *Chem. Des. Automation News* **1993**, *8*, 31−37.
(34) Cambridge Crystallographic Data Centre. The search for silylamido zirconium structures found the following structures: (**BUTTAL**) Planalp, R. P.; Andersen, R. A.; Zalkin, A. *Organometallics* **1983**, *2*, 16. (**CEBWAH**) Planalp, R. P.; Andersen, R. A. *Organometallics* **1983**, *2*, 1675. (**KIHRAU**) Bradley, D. C.; Chudzynska, H.; Backer-Dirks, J. D. J.; Hursthouse, M. B.; Ibrahim, A. A.; Motevalli, M.; Sullivan, A. C. *Polyhedron* **1990**, *9*, 1423.

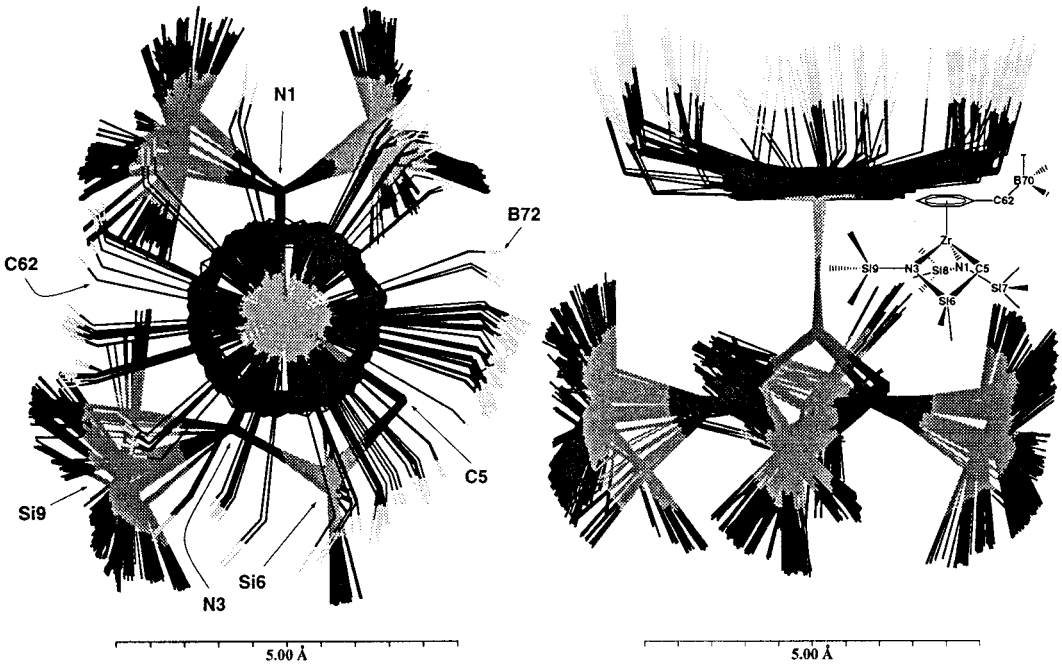

Figure 3. Overlay plot of the static ensemble viewed down the benzylic dummy atom−zirconium axis from the benzyl side (left) and viewed from the Si6 corner of the azasilametallocyclobutane ring. Hydrogens and the borate perfluoro phenyl rings have been hidden for clarity.

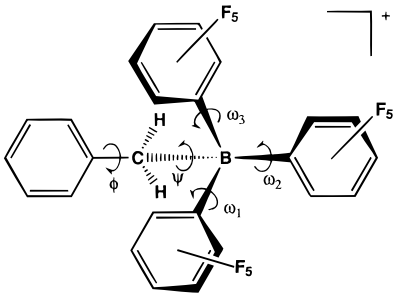

Figure 4. *M* or *P* conformation affects the ipso benzyl carbon torsion.

step is to find the conformer(s) that best account for the observed NOESY data. The inclusion of more than one conformation in NOE analysis will always lead to better agreement between computed and observed spectra. Thus, critical issues for the analysis of the benzylborato−azasilazirconacyclobutane complex, **1**, are (1) is it significant to use more than one conformation and (2) what is (are) the structure(s) of the conformer(s) that yield the best fit with the smallest number of significant conformer(s)? We address these issues by comparing the quality of the fit to the NOE data using the best set of one, two, or three conformers obtained by exhaustively searching all possible combinations of 204 trial conformations (corresponding to 204, 20 706, and 1 394 204 combinations, respectively).

The results with the 10 lowest *R*-factors resulting from single-conformer fit are shown in Table 1. The best fitting ($R = 1.069$) single structure solution is obtained with a conformation that has a Zr−DA distance of 2.26 Å and constrained improper torsions at N1 and N3. This conformation, which is illustrated in Figure 6, has the N1 silylmethyls pointing away from the benzyl ring and the N3's pointing toward the ring. Note the proximity of the benzylic carbon (C62) and metallacycle carbon (C5).

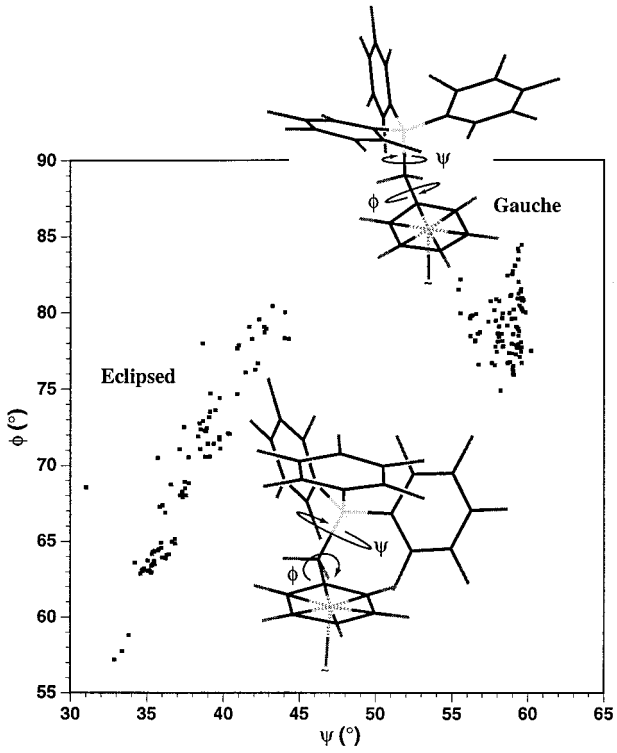

Figure 5. Correlation between the benzyl carbon−boron torsion, ψ, and the ipso benzyl carbon torsion, ϕ. The conformers on the left eclipse the benzyl ring with a perfluorophenyl ring. The conformers on the right have perfluorophenyl rings arranged gauche to the benzyl ring, and the ortho fluorine of the trans phenyl ring is between the two methylene hydrogens. Two *P* atropisomers are shown.

The best fit to a set of two static conformers ($R = 0.851$) is a 57:43 ratio of conformers where the major conformer has C62 proximal to C5, and in the minor conformer, the benzyl ring is rotated so that C62 is close

Table 1. Top 10 Solutions for Exhaustive Singles Fitting of the Static Ensemble

	conformer			
R-factor	Zr−DA (Å)	IT N1[a]	IT N3[b]	IT constr[c]
1.069	2.26	−	+	+
1.077	2.26	−	+	−
1.077	2.26	−	+	−
1.079	2.11	−	+	−
1.080	2.11	−	+	−
1.110	2.26	−	+	+
1.118	2.11	−	+	−
1.130	1.96	−	+	−
1.140	2.11	+	+	+
1.141	2.26	+	+	+

[a] The N1 improper torsion (IT) is defined using the IJKL method by N1−Si7−Si8−Zr2 and when shown as negative (−) orients the pendant $SiMe_3$ groups away from the benzylic ring. [b] The N3 improper torsion is defined as above by N3−Si9−Si6−Zr2 and when shown as positive (+) orients the pendant $SiMe_3$ group toward the benzylic ring. [c] When shown as positive (+), N1 and N3 improper torsions were constrained to ±3° and ±13°, respectively.

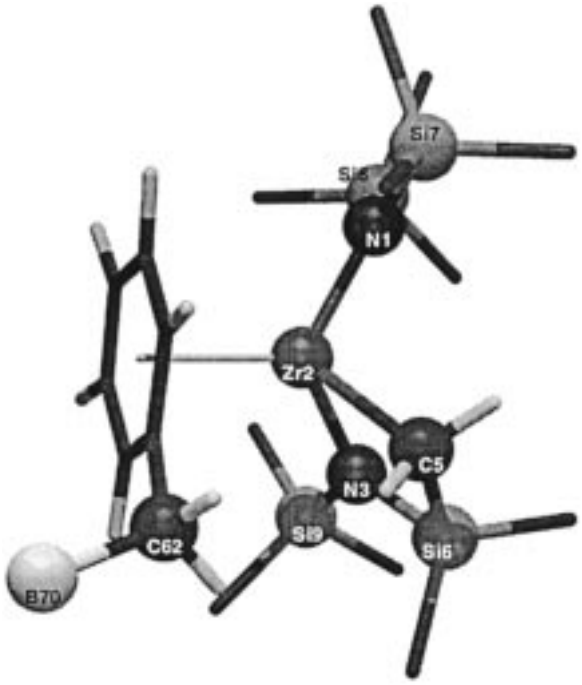

Figure 6. The best fit single static conformation and starting point for trajectory 11 from the dynamically averaged ensemble. The average of this trajectory participates (as the major conformer) in two of the five best dynamic doubles fits to the observed data. The perfluorophenyl rings and methyl hydrogens have been hidden for clarity.

to N1, as shown in Figure 7. This solution has the same silylamide configuration for both conformers; N1 and N3 are constrained to point their pendant silylmethyls toward the benzyl ring. Both conformers also have a Zr−DA distance of 2.26 Å. Table 2 gives the rest of the 10 best static doubles fitting results.

The best fitting set of three static conformers (R = 0.818) has a 43:37:20 ratio, consisting of the second best fitting doubles pair plus a minor conformer that is similar to the minor conformer of the best fitting double. Application of the *F*-test at the 95% confidence level indicates that it is statistically significant to use two rather than one static conformation in fitting the data but that three conformations do not lead to a significantly better fit relative to two conformations. The static triples solutions are otherwise unremarkable.

Conformer Populations from Dynamic Averaging. We (Landis and Wright) recently have detailed changes to the 2DCPA program that allow us to use a more physically realistic model of the NOE experiment by accommodating rapid (<10 ps lifetimes) local motion over short time scales.[24] Calculated NOE intensities are averaged in r^{-3} space during the course of 10 ps molecular dynamics trajectories. Computational efficiency is gained by only calculating trajectories using the best fitting static structures as starting points. This approach conserves the conformational and structural features that best fit the observed NMR data while minimizing the size of the dynamic ensemble.

A total of 22 conformers were selected for dynamic averaging as described in the Experimental Section. Each of the 22 trajectories was averaged over 1000 frames in 10 ps at 300 K. From these averaged trajectories, NOE time courses were computed and populated to give the best fit to experimental data.

An *R*-factor of 0.769 was obtained for the best fit using a single trajectory (trajectory number 13). This conformation has an equilibrium Zr−DA distance of 2.26 Å, the constrained silylmethyls of both N1 and N3 start out pointing toward the benzyl ring. As expected, N1 inverts rapidly during dynamics when constrained. The ipso benzylic methylene torsion (ϕ) is much less than 90°. An overlay plot representing trajectory number 13 is shown in Figure 8. By way of comparison, the fit obtained by holding this conformer static has an *R*-factor of 1.275. A similar extent of change in *R*-factors between static and dynamically averaged conformers is seen across the dynamic ensemble. It is also significant that the general ordering of the dynamic fits is not consistent with that of the static fits. *These results strongly suggest that large magnitude librations are occurring in solution, and even a multiconformational static model does not adequately describe the NOESY data.* Correspondingly, one should be cautious in interpreting NOE data when simple models are assumed.

Two conformer dynamic fitting yields the smallest *R*-factor of 0.671 for a structure that is 68% trajectory number 13 and 32% trajectory number 5. The force field for trajectory number 5 has an equilibrium Zr−DA distance of 2.26 Å and no constraints on the nitrogens. In this trajectory the silylmethyls of N1 are oriented toward the benzyl ring and the pendant silylmethyl of N3 is pointing toward the ring. The ipso benzylic methylene torsion (ϕ) is much less than 90°. An overlay plot representing trajectory number 5 is shown in Figure 8. Again, for comparisons' sake, static doubles fitting of the starting conformers of trajectories 13 and 5 results in an *R*-factor of 1.061. In the static fitting, the starting point of trajectory number 13 is again the majority of the 54:46 mixture.

Application of the *F*-test at the 99.99% confidence level for each combination of the 10 best dynamically averaged doubles and singles fits indicates that it is statistically significant to use two rather than one conformation in fitting the data. In contrast, the best three trajectory combinations do not lead to a signifi-

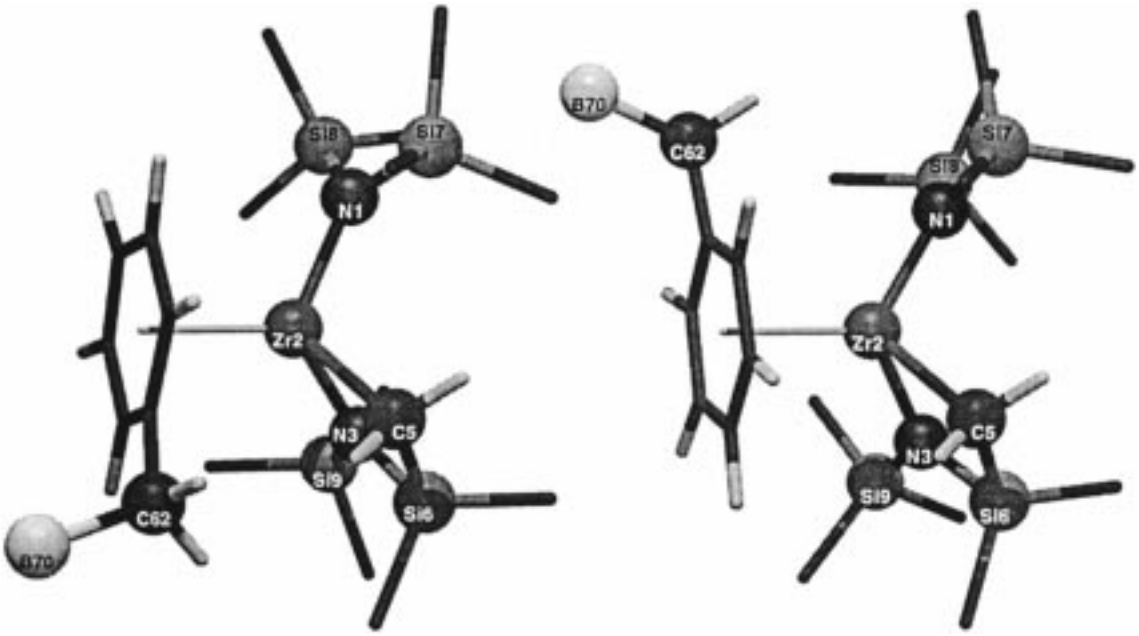

Figure 7. The major (left) and minor (right) conformers from the best static fit using two conformations. The perfluorophenyl rings and methyl hydrogens have been hidden for clarity.

Table 2. Top 10 Solutions for Exhaustive Doubles Fitting of the Static Ensemble

	conformer 1				conformer 2				
R-factor	Zr−DA (Å)	IT N1[a]	IT N3[b]	IT constr[c]	Zr−DA (Å)	IT N1[a]	IT N3[b]	IT constr[c]	weight
0.851	2.26	+	+	+	2.26	+	+	+	57−43
0.854	2.11	+	−	−	2.26	+	+	+	55−45
0.858	2.26	+	−	−	2.26	+	+	+	55−45
0.860	2.26	+	+	+	2.26	−	+	−	57−43
0.861	2.26	+	−	−	2.26	+	+	+	54−46
0.862	1.96	+	−	−	2.26	+	+	+	57−43
0.869	1.96	−	+	+	2.26	+	+	+	61−39
0.869	2.11	+	−	−	2.26	−	+	−	55−45
0.872	2.26	+	+	+	2.11	+	+	+	60−40
0.873	1.96	+	+	−	2.26	−	+	−	57−43

[a] The N1 improper torsion (IT) is defined using the IJKL method by N1−Si7−Si8−Zr2 and when shown as negative (−) orients the pendant $SiMe_3$ groups away from the benzylic ring. [b] The N3 improper torsion is defined as above by N3−Si9−Si6−Zr2 and when shown as positive (+) orients the pendant $SiMe_3$ group toward the benzylic ring. [c] When shown as positive (+), N1 and N3 improper torsions were constrained to ±3° and ±13°, respectively.

cantly better fit vis-à-vis the best two trajectory solutions.

Significant Conformations. In general, we find that the *R*-factor for the fitting of the data is sensitive to the details of the benzyl borate coordination geometry. The data also support a distinction between the two possible configurations of each of the silylamides, but not the determination of a precise (i.e., at higher resolution than ca. 10°) improper torsion angle. Figure 9 shows that the dynamically averaged conformations that best fit the experimental data span a range of benzylic torsions from approximately −45° to 150° in two broad distributions. In our experience, only a dynamic approach to this range of motion will produce satisfactory results. The best fits are consistent with **1** exchanging between two broad, distinct minima on the ring rotation potential energy surface across a small but nonnegligible barrier.

The features that are conserved among the best dynamically averaged two-conformer fits are (1) the inadequacy of static conformations to account for the observed data, (2) a major population that eclipses the metallocyclobutylmethylene (C5) with the benzylic methylene (C62), (3) a minor population that eclipses the free silylamide (N1) with C62, (4) a zirconium to benzyl ring dummy atom distance in the range 2.11−2.26 Å, (5) the orientation of the pendant silylmethyls of N3 toward the benzyl ring, (6) the nearly planar configuration of N1, and (7) the ipso benzylic methylene torsion (ϕ) being much less than 90°.

Conclusions

We have demonstrated that solution structures of organometallic complexes can be modeled provided that care is taken in the quantifying the NOE data and in choosing physical realistic models for the data analysis. We find that **1** is best modeled as rapidly exchanging between two conformer populations whose most important difference is the orientation of the trisperfluorophenyl benzyl borate anion on the asymmetric coordination site. A mixture of static conformations does not satisfactorily explain the observed spectra. It is necessary to invoke a dynamic representation of **1** to account for experimental NOE data. This case underscores the need to evaluate critically the validity of computational models and to improve on the fidelity of NOE simulations. In particular, one is cautioned against overinter-

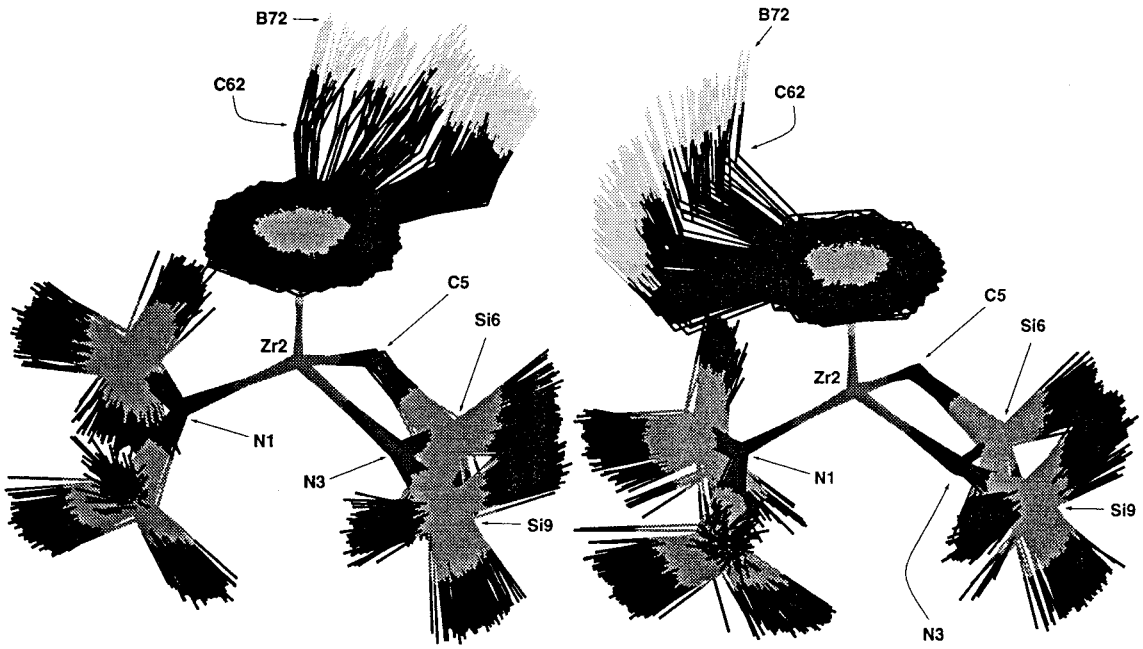

Figure 8. Dynamics averaging (shown every 0.2 ps) of conformer 13 (left) and conformer 5 (right) from the dynamics-averaged ensemble. The perfluorophenyl rings and hydrogens have been hidden for clarity.

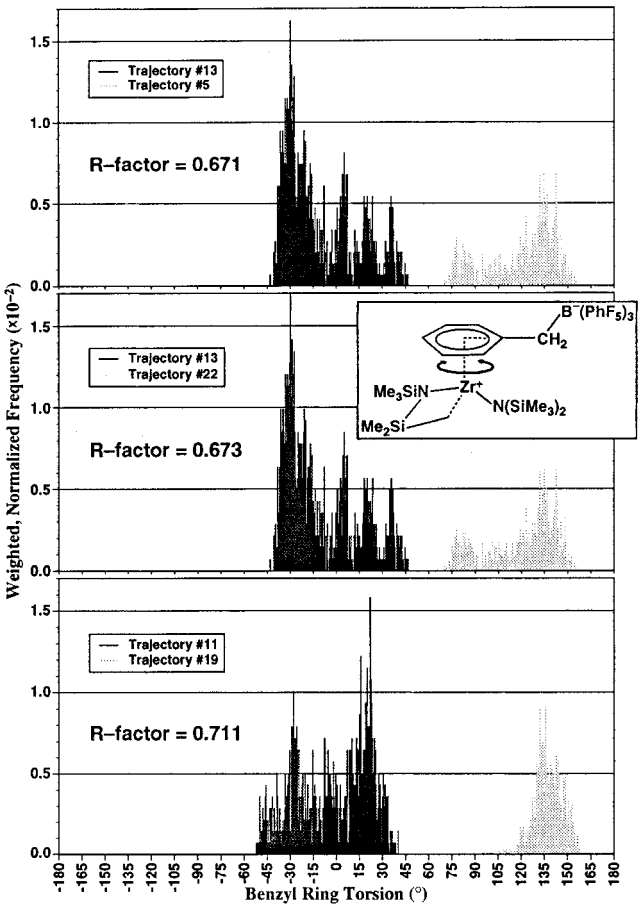

Figure 9. Torsional distributions for the benzylic ring in the best, second best, and 13th dynamic two-conformer fits. The 13th fit is the best that does not contain any trajectory from the best two (13, 5, or 22). The major conformer population is shown in the dark color.

preting qualitative NOE data in terms of a single structure, especially when the molecules are conformationally supple.

The results suggest that the major population is one in which the benzylic methylene eclipses the azasilametallocyclobutyl methylene and that in the minor population the benzylic methylene eclipses free silylamide nitrogen. The benzyl group is coordinated to the zirconium in both the major and minor populations. This conclusion supports the proposition that the low ethylene polymerization activity of the catalyst is due to tight binding of the borate. We conclude that the bis(trimethylsilyl)amido N is approximately planar and the annular amide exhibits some pyramidalization with its silylmethyls close to the coordinated benzyl ring of the borate. This conclusion suggests that the amide nitrogens retain a configuration in solution that is consistent with analogous X-ray crystal structures.

Experimental and Computational Methods Section

Molecular Modeling and Ancillary Programs. All the molecular mechanics computations that are discussed here were accomplished using the Molecular Classical Mechanics (MCM) suite of programs that encompass Rappe's Universal Force Field.[35] The scripting capability in SYBYL (SPL) was used to create a series of atropisomers of the triphenylborate and to reduce the size of the original search results set to a manageable ensemble by clustering.[36] Crystallographic data for parametrization was obtained from the Cambridge Structural Database using the Quest program.[33,37]

The graphing and conformer analysis capability of Cerius[2] aided in the interpretation of the ensemble.[38] Several of the molecular illustrations were prepared using modified versions of MOLSCRIPT[39] and Raster3D.[40,41]

(35) Rappe, A. K.; Casewit, C. J.; Colwell, K. S.; Goddard, W. A.; Skiff, W. M. *J. Am. Chem. Soc.* **1992**, *114*, 24−35.
(36) *Tripos*, 6.2 ed.; Tripos, Inc.: St. Louis, MO.
(37) *Cambridge Crystallographic Data Centre*, 1995 ed.; Cambridge Crystallographic Data Centre: Cambridge, England, 1995.
(38) *MSI*, 2.0 ed.; Molecular Simulations, Inc.: San Diego, CA.
(39) Kraulis, P. J. *J. Appl. Crystallogr.* **1991**, *24*, 946−950.
(40) Bacon, D.; Anderson, W. F. *J. Mol. Graphics* **1988**, *6*, 219−220.

2D NOESY Spectra. ^{1}H NOESY spectra (500 MHz) were obtained at 253 K in $CDCl_2CDCl_2$ with mixing times of 60, 150, 200, 300, 500, and 1000 ms. Spectra were gathered using the 2D-NOESY pulse sequence[42] and TPPI mode[43] without a homospoil pulse or random mixing variation. Data sets with t_1 and t_2 dimensions of 512 and 2048 real points, respectively, were collected using relaxation delays of 2.0 s for eight scans of each FID.

The XWINNMR[44] software package from Bruker was used to transform and process the data. t_1 and t_2 were used without zero-filling. t_2 was subject to dc offset correction, forward linear prediction, apodization of the last 60% of the data with a decaying cosine squared function, and convolution with a Lorentzian window of 1.5 Hz line width. t_1 was processed with forward linear prediction and cosine squared apodization, and without dc offset correction.

Following final phase and baseline correction in each dimension, t_1 noise was attenuated using mean-row subtraction[45] in Bruker's AURELIA program.[46,47] AURELIA was also used to compute the volume integrals by iterative segmentation through 100 iterations with a segmentation level of 20% of the peak height.

Peak assignments were based on the previous work by Horton and de With.[14] Qualitative NOE intensity resolved the ambiguity regarding peak assignments of the inequivalent methylenes and benzylic protons. To avoid biasing the results, these assignments were tested as detailed below.

Once the volumes of all the cross-peaks have been measured for each experimental mixing time, the intensity at zero mixing time is extrapolated for the diagonal cross-peaks. Examples are provided in the Supporting Information.The off-diagonal peaks are zero at zero mixing time. Together, the observed and extrapolated intensities provide the quantitative time course of NOE buildup. For off-diagonal peaks, the intensities of the two symmetry-related peaks were averaged prior to normalization.

Creation of the Static Conformational Ensemble for 2DCPA. An initial static ensemble of 204 model conformations (17 conformations selected from each of 12 classes) was generated with the program *uff*, which is part of the MCM package, using UFF as the force field. In all cases, charges were set to zero and no charge equilibration was used. The models do not take Coulombic interactions into account because *qeq2*, the charge equilibration program, gave chemically unreasonable charges in the zwitterionic complex (negative charge on the zirconium and positive charges on the boron and fluorines). A new atom type for η^6-bound arenes had to be created for the benzyl dummy atom in the model of **1**. The only differences between this new atom type, named PhR, and the standard *uff* Cp centroid dummy atom type, CpR, are in the equilibrium geometries; the force constants are unchanged. The new equilibrium distance between dummy atom and defining atoms is 1.173 vs 1.400 Å, and the size of the equilibrium angles involving the dummy atom and the defining atoms are 60° and 60° as opposed to 54° and 72°.

Initially, four independent starting conformers were created by sketching in the models for **1** with each of the possible inversions for N1 and N3. Once these models were well minimized (|grad| $\approx 10^{-10}$ kcal/(mol Å)), two distance constraints (10^4 kcal/(mol Å^2) force constant) were created to force the (Zr3+4)−(PhR) bond length to 2.26 and 1.95 Å. The distances are ±0.15 Å from the average distance found in the models minimized using the rule-based length generated by UFF. These constraints were used to minimize the default geometries for each starting inversion of N1 and N3. The set of three bond lengths serves to bracket the median distance of a survey of η^6 zirconocenes in the Cambridge Structural Database,[33] which was found to be 2.123 ± 0.098 Å in the nine structural analogues.[48]

While creating the first set of 12 conformers, it appeared that the nitrogens were far too pyramidal given their sp^2 N_2 atom type. The average inversion angles for the structures minimized at the default, explicit equilibrium value of 0° (0 kcal/mol force constant[35] for N) are 35° for N3 and 32° for N1. To correct for these exaggerated pyramidalization of the nitrogens, bond orders of 1.5 and 1.25 were used for N−Zr and N−Si bonds, respectively.

N1 was constrained to the smaller inversion in either direction of the improper torsion. The N1 improper torsion is defined using the IJKL method by N1−Si7−Si8−Zr2 and when positive orients the pendant $SiMe_3$ groups toward the benzylic ring. The N3 inversion, however, changed sign while being minimized under constraint, if the starting geometry had a negative sign. The N3 improper torsion is defined as above by N3−Si9−Si6−Zr2 and when positive orients the pendant $SiMe_3$ group toward the benzylic ring. The program *uff* does not have a true improper torsion constraint; instead, it has an inversion constraint where the only adjustable parameters are the height of the barrier between invertomers and the magnitude of their equilibrium inversion angles (ω_0). UFF constraints do not allow the vector of the inversion constraint to be specified, only the magnitude. Despite experimenting with very high barriers (10^9 kcal/mol), the minimizer always carried N3 over to negative improper torsions. When inversions of N3 are negative, only large-magnitude deflections (>25°) avoid severe steric congestion with the silylmethyls of N1. It appeared to be impossible to retain both configurations at N3 when the ω_0 was less than 15°. This observation suggests that conformations possessing small, negative, improper torsions at N3 can be safely neglected.

Thus, the starting set for the torsional search used to generate the conformational ensemble consisted of 3 Zr−PhR distances + 2 N1 invertomers + 2 N3 invertomers = 12 classes. With 6 of the classes divided into subclasses (nitrogens constrained and unconstrained both N1's and one N3), 18 well-minimized (|grad| $\approx 10^{-10}$ kcal/(mol Å)) models were created, each with its unique set of constraints.

This set of 18 models was searched for new rotamers in the *uffsrch* program of the MCM suite. This program automates searches of torsion angle space and was set to collect 30 conformers using the protocol outlined in Table 3. Rotatable bonds that would move nonequivalent hydrogens were searched by a combination of incremental, random, and energy-directed means; for example, methylene but not methyl rotations were searched. A range of C56−C62 torsion values was searched that would keep the borate and the zirconium on opposite sides of the benzyl ring plane. Each of the resulting 540 conformers was minimized using 1000 steps of conjugate gradient mini-

(41) Merritt, E. A.; Murphy, M. E. P. *Acta Crystallogr., Sect. D: Biol. Crystallogr.* **1994**, *50*, 869−873.
(42) Macura, S.; Ernst, R. R. *Mol. Phys.* **1980**, *41*, 95−117.
(43) Marion, D.; Wüthrich, K. *Biochem. Biophys. Res. Commun.* **1983**, *113*, 967−974.
(44) *XWINNMR*, 1.2 ed.; Bruker Analytische Messtechnik GmbH: Rheinstetten.
(45) Klevit, R. E. *J. Magn. Reson.* **1985**, *62*, 551−555.
(46) *AURELIA*, 941101 ed.; Bruker Analytische Messtechnik GmbH: Rheinstetten.
(47) Neidig, K. P.; Geyer, M.; Görler, A.; Antz, C.; Saffrich, R.; Beneicke, W.; Kalbitzer, H. R. *J. Biomol. NMR* **1995**, *6*, 255−270.
(48) Cambridge Crystallographic Data Centre. The search for η^6 zirconocene structures found the following structures: (**CLZRAL**) Stollmaier, F.; Thewalt, U. *J. Organomet. Chem.* **1981**, *208*, 327. (**JISLEC**) Troyanov, S. I.; Rybakov, V. B. *Metalloorg. Khim. (Organomet. Chem. USSR)* **1989**, *2*, 1382. (**JISLIG**) Troyanov, S. I.; Rybakov, V. B. *Metalloorg. Khim. (Organomet. Chem. USSR)* **1989**, *2*, 1382. (**PAVLUT**) Pellecchia, C.; Grassi, A.; Immirzi, A. *J. Am. Chem. Soc.* **1993**, *115*, 1160. (**PENSEG**) Troyanov, S. I.; Rybakov, V. B. *Metalloorg. Khim. (Organomet. Chem. USSR)* **1992**, *5*, 1082. (**PENSIK**) Troyanov, S. I.; Rybakov, V. B. *Metalloorg. Khim. (Organomet. Chem. USSR)* **1992**, *5*, 1082. (**TAMCUF**) Cotton, F. A.; Kibala, P. A.; Shang, M.; Wojtczak, W. A. *Organometallics* **1991**, *10*, 2626. (**VOSVAA1**) Diamond, G. M.; Green, M. L. H.; Walker, N. M.; Howard, J. A. K.; Mason, S. A. *J. Chem. Soc., Dalton Trans.* **1992**, 2641. (**WEXSOH**) Cotton, F. A.; Wojtczak, W. A. *Inorg. Chim. Acta* **1994**, *217*, 187.

Table 3. Torsional Search Scheme

atom 1[a]	atom 2[a]	search method	steps[b]
Zr2	PhR4	exhaustive	24
N1	Si8	systematic, discrete	FF torsional space
N1	Si7	systematic, discrete	FF torsional space
C56	C62	systematic, discrete	FF torsional space
Zr2	N1	systematic, discrete	FF torsional space
N3	Si9	systematic, discrete	FF torsional space

[a] The torsions are selected using the ends of the rotatable bond, and the bonds were picked in this order to minimize the apparent change in overall orientation of the molecule. [b] *uffsrch* exhaustive searching is an incremental, 360° search from the starting torsion. Discrete systematic searching sets the torsion to the minima in that bond's torsional energy term as set by the force field.

mization with a gradient cutoff of 10^{-1} kcal/(mol Å) to remove bad steric contacts. Next, each conformer was subject to as many steps of quasi-Newton−Raphson minimization as were required to reach a gradient of less than 10^{-2} kcal/(mol Å).

All 540 of the minimized conformations were created starting from the *P* atropisomer[29] of the trisperfluorophenyl borate. An additional 540 conformers were created by exchanging the magnitude and signs of the torsions that describe the phenyl rotation of the two perfluorophenyl borate rings that are farthest from the η^6 benzyl ring. This second set of 540, mostly *M* atropisomer, conformations were then minimized as above.

Experience has shown that a reasonable initial ensemble for 2DCPA is about 200 conformers. As a result, it was necessary to select a subset of the 1180 conformations while still spanning as much of the conformational space as possible. Clustering, as described fully in the Supporting Information, was used to decrease the ensemble size to 200 representative conformers.

Model Relaxation Parameter Optimization. Once the NOESYs have been collected and the static ensemble has been generated, *2DCPA* requires three parameters for operation: the isotropic rotational correlation time (τ_{iso}), the methyl rotational correlation time (τ_{Me}), and the external relaxation rate (R_{ext}). These parameters are determined by minimizing a fitting error function, computed like the *R*-factor, for a select subset of the calculated and experimental NOESY peaks. 2DCPA can automatically optimize the three parameters either sequentially or simultaneously. In this case the parameters had to be optimized sequentially because simultaneous optimization would not converge on a solution for many of the conformers.

We started by adjusting τ_{iso}, then R_{ext} was optimized, and finally τ_{Me}, which has been the least sensitive of the three parameters in our experience. For computations in the fast exchange limit, such as this one, it is not strictly necessary to optimize R_{ext} because it only affects the diagonal cross-peaks, which are not considered (0 weight) in the usual computation of the fit to experimental data. The global optimum for each parameter was the median value of the optima for all the conformers in the static ensemble. Optimization of τ_{iso} and τ_{Me} was repeated sequentially four times until their value did not change.

The ideal cross-peak for optimization is one in which the interproton distance is independent of the conformation. It is even better when at least one ideal cross-peak representing each possible combination of methyl and nonmethyl protons is available. The protons selected for optimization are detailed in the Supporting Information. Final values used in the calculations are shown in Table 4.

Conformer Population Analysis of the Static Ensemble. The static ensemble was exhaustively fitted with each possible single-, double-, and triple-conformer solution in the fast exchange mode. Multiconformational solutions with less than 0.01% contribution of a conformer were rejected as insignificant. Any solution with an *R*-factor greater than 3.0 was not reported. Significance testing was done using Hamilton's *F*-test on every possible combination of the 10 lowest *R*-factor single, double, and triple static fits.

Table 4. Model Relaxation Parameters for the Static Ensemble

τ_{iso} (ns)	τ_{Me} (ps)	R_{ext} (s)	τ optimizer mode	τ optimizer cutoff
1.25	155	0.0	0	1.0×10^{-4}

Table 5. Model Relaxation Parameters for the Dynamics Ensemble

τ_{iso} (ns)	τ_{Me} (ps)	R_{ext} (s)	τ optimizer mode	τ optimizer cutoff
1.236	128	0.0	0	1.0×10^{-4}

Verifying Peak Assignments Based on Qualitative NOESY Data. Because qualitative NOE intensities were used to resolve the ambiguity in assigning two diastereotopic sets of peaks (the dimethylsilyl methyl groups and the diastereotopic ortho and meta protons of the benzyl arene ring), the assignments were tested by swapping groups in the input file, reoptimizing the model relaxation parameters, and checking the value of the lowest *R*-factor singles fits. The quality of the best fits declined in both cases, indicating correct initial assignment of the peaks.

Creation of the Dynamically Averaged Conformational Ensemble for 2DCPA. The starting points for dynamics trajectories were selected from the 10 best fits (less duplications) in each of the static singles, doubles, and triples *2DCPA* runs. The dynamics simulations for averaging were run using the *md* program of MCM at 300 K. The adiabatic simulations were isoergic, isochoric, standard Verlet dynamics with a time step of 1 fs, recorded every 10 fs for 10 ps (1000 frames). The temperature scaling window was ±20 K.

Conformer Population Analysis of the Dynamically Averaged Ensemble. A total of 22 conformations were used as starting points for short dynamics trajectories. These conformers came from the nonredundant list of the top 10 conformers from single, double, and triple static fits. The 22 conformers were selected without regard to their force field, that is, Zr−PhR distance, nitrogen configuration, or nitrogen constraints. Each of the 22 trajectories was averaged over 1000 frames in 10 ps at 300 K. The model relaxation parameters were reoptimized for use with the dynamics ensemble and are shown in Table 5.

One functional change has been made to the *2DCPAavg* program since the last publication detailing its operation.[24] The program has been split into two components, *2DCPArm6* and *2DCPAavg*, and a third program, *2DCPAavgopt*, has been added. *2DCPArm6* handles averaging the coordinates in r^{-3} space and averaging the spherical harmonic contributions of methyl groups in $\cos^2(\theta)$, $\sin^2(\theta) + \cos^2(\theta)$, and $\sin^2(\theta)$ angular spaces. *2DCPArm6* creates an intermediate file to store the averages for all the input trajectories. This change was made so that *2DCPAavgopt* could share the averages with *2DCPAavg* and avoid time-consuming recalculation. *2DCPAavgopt* uses the same optimization algorithm as *2DCPA* to find values for the model isotropic rotational correlation time, methyl rotational correlation time, and external relaxation rate that minimize the fitting error with selected peaks. Once *2DCPAavgopt* has found the model relaxation parameters, *2DCPAavg* uses the modified input to calculate and save either apparent intensities or apparent rates as previously described.[24]

The dynamics trajectory input program, *2DCPArm6*, read in the list of dynamics trajectories and, in turn, averaged each set of coordinates in r^{-3} space and the spherical harmonic contributions of methyl groups in angular spaces. The resulting spatial averages were stored as an intermediate file for use by the *2DCPAavgopt* and *2DCPAavg* programs. The *2DCPAavgopt* program was then used to read in the averages

for each conformer and optimize the model relaxation parameters as described for the static ensemble. The resulting parameters were transferred to a new input file for *2DCPAavg*.

Once the model relaxation parameters are determined, the dynamic averaging program, *2DCPAavg*, read in the new dynamic input file and spatial averages files, computed the apparent rates for each conformer, and stored the results for use by the *2DCPA* program. This rate ensemble was then exhaustively fitted with every possible single-, double-, and triple-conformer solution in the fast exchange mode. Multiconformational solutions with less than 0.01% contribution of a conformer were rejected as insignificant. Any solution with an *R*-factor greater than 3.0 was not reported. Hamilton's *F*-test was applied to every possible combination of the 10 best resulting singles, doubles, and triples fits for 366 observations.

A complete ".csr" format (Quanta) trajectory file of the static ensemble and all 22 ".trj" format (Polygraf) dynamics trajectory files are available on request from Landis.

Acknowledgment. Partial financial support from the DOE and NSF is gratefully acknowledged. J.M.W. thanks Royal Dutch/Shell for the "stagiare" (internship) appointment and financial support under the direction of Dr. Geoffrey J. Nesbitt. We thank Prof. Edwin L. Sibert for helpful discussions concerning matrix algorithms and Dr. Mike A. King for training on SYBYL and clustering.

Supporting Information Available: Supporting materials include the atom-numbering scheme used to describe **1**, all NOE data, and descriptions of the conformational ensembles (9 pages). Ordering information is given on any current masthead page.

OM980571O